GAMMA DETECTORS FOR EXPLOSIVE AND DRUG DETECTION SYSTEMS

V.M. Bystritsky, E.V. Zubarev, A.V. Krasnoperov, S.Yu. Porokhovoy, V.L. Rapatsky, Yu.N. Rogov, A.B. Sadovky, A.V. Salamatin, R.A. Salmin V.M. Slepnev (Joint Institute for Nuclear Research, Russia), *E.A. Andreev* (*Neutron Technologies*, Russia)

Abstract
The Joint Institute for Nuclear Research (JINR) has developed and fabricated BGO-based γ-detectors that are used in explosive and drug detection systems. The detector design and main characteristics are addressed. The method for software temperature stabilization of γ-detector response is described that allows operating the detector in a temperature range from -20 ^{0}C to 50 ^{0}C.

1. Introduction

The Joint Institute for Nuclear Research developed and manufactured several experimental systems for detection and identification of hidden explosives and drugs [1 - 3] based on the tagged neutron method (TNM).

The elemental composition of an object under investigation is determined through detection of characteristic γ-rays produced in the process of inelastic scattering *A(n,n')A* of 14.1 MeV fast neutrons on nuclei of an irradiated sample. ING-27[4] neutron generator serves as a source of 14.1 MeV neutrons produced in the binary reaction *t(d,n)α*.

Let's formulate the main requirements that a γ-detector must satisfy:

- high efficiency of γ-ray detection in an energy range from 1 to 10 MeV;
- low sensitivity to the neutron background in relation to efficiency of γ-ray detection;
- linear response;
- good energy and time resolution in the specified γ-ray energy range;
- short scintillator decay time;
- radiation resistance and stability of parameters with time.

Currently detectors based on inorganic scintillators are used most frequently for detection of gamma radiation in the above specified energy range.

2. Inorganic Scintillators Employed in TNM

A detailed overview of properties of scintillators used for gamma-radiation detection in a wide energy range can be found in [5, 6, 7]. This paper is concerned with properties of scintillators that found application in explosive and drug detection systems using the tagged neutron method. Table 1 [8] lists the main characteristics of γ-ray detectors.

Table 1

Scintillator characteristics

Type / Properties	NaI(Tl)	BGO	$LaBr_3$(Ce)
Density, g/cm^3	3.67	7.13	5.29
Effective atomic number, Z	50	75	47
Radiation length, cm	2.59	1.12	1.88
Decay time, ns	245	300	20

Wavelength in the spectrum maximum, nm	410	480	356
Relative light output, %	100	21	130
Refraction factor	1.85	2.15	1.9
Melting temperature, ^{o}C	651	1050	788
Radiation resistance, Gy	10^3	10^3-10^4	-
Hygroscopicity	Yes	No	Yes

2.1. Sodium Iodide (NaI(Tl))

Currently sodium iodide activated with thallium is one of the most widespread scintillators used for γ-ray detection. Its distinguishing feature is high light output that determines relative energy resolution of the order of ~7%[1] for crystals of small size.

Owing to good energy resolution and availability, NaI(Tl) γ-detectors are widely used in TNM, particularly in stationary setups for inspection of large-sized cargoes [9, 10]. Dependence of the efficiency of 4439 keV γ-ray detection (full-energy peak efficiency) on the size of a crystal is presented in [10, 11] (explosive and drug identification is based on analysis of the characteristic radiation of carbon, nitrogen and oxygen nuclei with energies of 4439, 5100 и 6130 keV). The efficiency of γ-ray detection by a detector with a NaI(Tl) crystal the size of 5"×5" is by 6.5 times more than the corresponding value for a 3"×3" crystal. Among NaI(Tl) disadvantages are its hygroscopicity and fragility, which restricts its application in hand-held inspection systems. NaI(Tl) crystals possess the lowest efficiency of γ-ray detection at higher sensitivity to the neutron background as compared with other scintillators of the same size listed in Table 1.

2.2. Lanthanum Bromide ($LaBr_3$(Ce))

Characteristics of $LaBr_3$(Ce) γ-detectors for γ-ray detection in systems using TNM were studied in [12] and [13]. This crystal has large light output and the best energy resolution (~2.9 % on the 662 keV line [12]) in comparison with NaI(Tl) crystal. The short decay time makes it possible to employ γ-detectors at high count rate of the detected events without significant deterioration of their energy resolution The time resolution of the system for detection of (α-γ)-coincidences (a silicon detector is used as an α-detector and $LaBr_3$(Ce) detector – as a γ-ray detector) is ~1.1 ns [13].

2.3. Bismuth Germanate (BGO)

Owing to high density and a large atomic number, BGO detectors possess the greatest efficiency of γ-ray detection as compared with the crystals listed in Table 1. Dependence of the efficiency of γ-ray detection (full-energy peak efficiency) on the energy of γ-rays is presented for three crystals of the same size in Table 2.

Table 2

Efficiency of detection (full-energy peak efficiency) of γ-rays with energies of 0.368, 1.33 and 6 MeV in relation to efficiency of detection of 1.33 MeV γ-rays by NaI detector [12]

Energy / Crystal	368 keV	1.33 MeV	6 MeV
NaI (3"×3")	2.822	1.000	0.259
$LaBr_3$ (3"×3")	2.941	1.362	0.457
BGO (3"×3")	3.587	2.514	1.363

[1] full width at half maximum by the full-energy peak of 662 keV γ-rays

2.3.1. Gamma-Detector Design

Fig. 1. Outward appearance of γ-detector

Fig. 1 shows a complete gamma-detector. BGO crystal is a cylinder of Ø76×65 mm. Hamamatsu R6233-100 with a gain factor ~2.3×105 and supply voltage ~1000 V is used as a photomultiplier tube (PMT). A light contact between the PMT input window and the BGO end surface is covered with optically transparent epoxy adhesive. TMP36 analog temperature sensor monitors the crystal temperature [14].

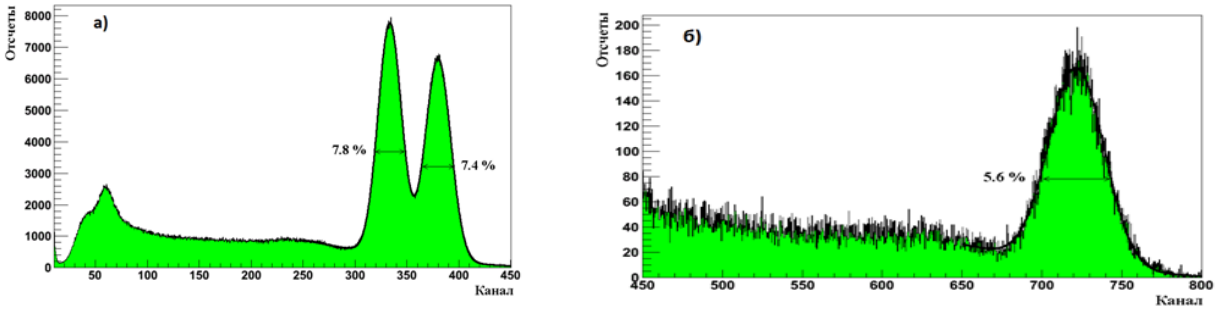

Fig. 2. Amplitude spectrum of 60Co isotope. Full-energy peaks of 1173 and 1332 keV γ-rays (a) and the total peak corresponding to the energy of 2505 keV at simultaneous detection by a detector of two γ-rays (b). The line indicates the result of peak approximation to the Gaussian function. The background substrate under the peak was described by a linear function

2.3.2. Gamma-Detector Characteristics

Linearity of the detector response and its energy resolution in the energy region from 0.5 to 2.6 MeV were determined using the lines of γ-rays of standard set isotopes RSGS[2]. The width of γ-ray full-energy peaks (Table 3) and the maximum position in the amplitude spectrum were determined based on their approximation to the Gaussian function. The background substrate under the peak was described by a linear function. The measured dependence of the amplitude of BGO light output amplitude on the energy of γ-rays is described by a straight line with better accuracy than 0.4 %.

[2] Reference spectrometric gamma-ray sources

Table 3

Sources of γ-radiation and γ-ray energy

Isotope	^{228}Th	^{228}Th	^{137}Cs	^{54}Mn	^{60}Co	^{60}Co	^{40}K	^{60}Co	^{228}Th
E_γ, кэВ	511	583	662	835	1173	1332	1461	1173+1332	2615

Fig. 2 (a, b) shows amplitude spectra of events detected by a γ-detector exposed to ^{60}Co source.

For γ-ray energies above 2.6 MeV the response linearity was checked directly by the energy spectra of γ-rays produced at irradiation by fast neutrons of samples of pure carbon and dummy explosive - melamine ($C_3H_6N_3$). In the energy range from 2.6 to 6.1 MeV a deviation from linearity does no exceed 0.35%.

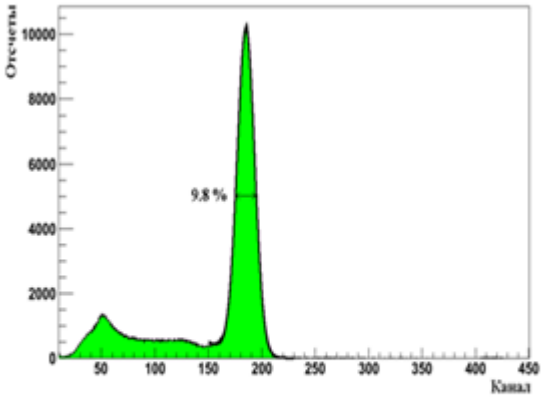

Fig. 3. Amplitude spectrum of ^{137}Cs isotope. The line indicates the result of approximation of 662 keV γ-ray full-energy peak to the Gaussian function. The background substrate under the peak is described by a linear function

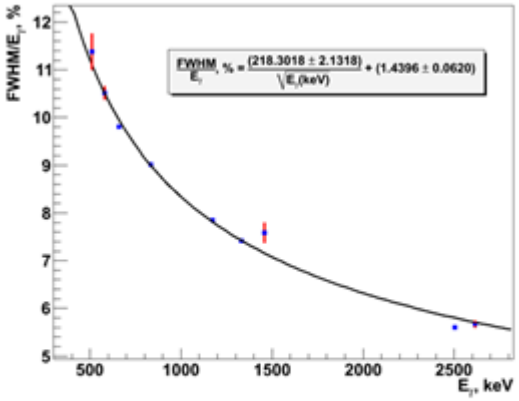

Fig. 4. The measured dependence of the detector relative energy resolution on the γ-ray energy (dots) and its approximation to the function of the type ~$E^{-0,5}$ (line)

Relative energy resolution of a γ-detector for ^{137}Cs isotope is 9.8% (Fig. 3) and 7.8 % and 7.4 %, respectively, if the detector is irradiated by γ-rays with energies of 1173 and 1332 (Co^{60} peaks). Fig. 4 presents dependence of the detector resolution on the γ-ray energy. The measured dependence is described with a good accuracy by the expression of the type ~$E^{-0.5}$.

The amplitude distribution of events detected by a γ-detector at irradiation by a fast neutron flux of a ^{12}C sample is given in Fig. 5 (a). The positions and widths of peaks with energies of 4438 keV and 3927 keV (peak of a single escape of 511 keV γ-rays) were determined through approximation to the Gaussian function. The energy resolution of a γ-detector on the 4438 keV line amounts to 4.6 %.

Fig. 5 (B) shows the spectrum of time intervals between detections of a γ-ray of carbon nuclei characteristic radiation measured in coincidences with a signal from an α-detector. The time resolution of the system for detection of (α-γ)-coincidences is 3.2 ns.

3. Temperature Stabilization of Gamma-Detector Response

When operating BGO γ-detectors, it is necessary to take into account a sufficiently sharp temperature dependence of the light output and the crystal decay time. When the temperature of a crystal changes from 0 to 40 °C, the duration of scintillation flash decreases from 400 to 200 ns and the light output drops by more than two times [6]. The temperature factor of light output variation depends on the crystal quality and lies in the range from 1 to 1.6 %/°C.

Stabilization of energy calibration depending on the light output can be attained through crystal thermostatic temperature control. This method found application in laboratory measurements and in experiments on accelerators and reactors with the use of large-sized stationary detecting systems. In particular, the developed cooling system [15] of and electromagnetic calorimeter in the L3 experiment carried out on the LEP accelerator at (CERN, Geneva) maintained the temperature of over 11000 BGO crystals in the range from 17 to 18 °C during the whole time of the system operation.

Application of temperature stabilization devices of γ-detectors in portable and mobile inspection systems for explosive and drug detection is not feasible because of significant restrictions on dimensions and weights of these systems. An alternative method for solving the problem related to stabilization of energy calibration of a channel detecting characteristic nuclear gamma-radiation is a method for correction of γ–detector amplitude response depending on the BGO crystal temperature.

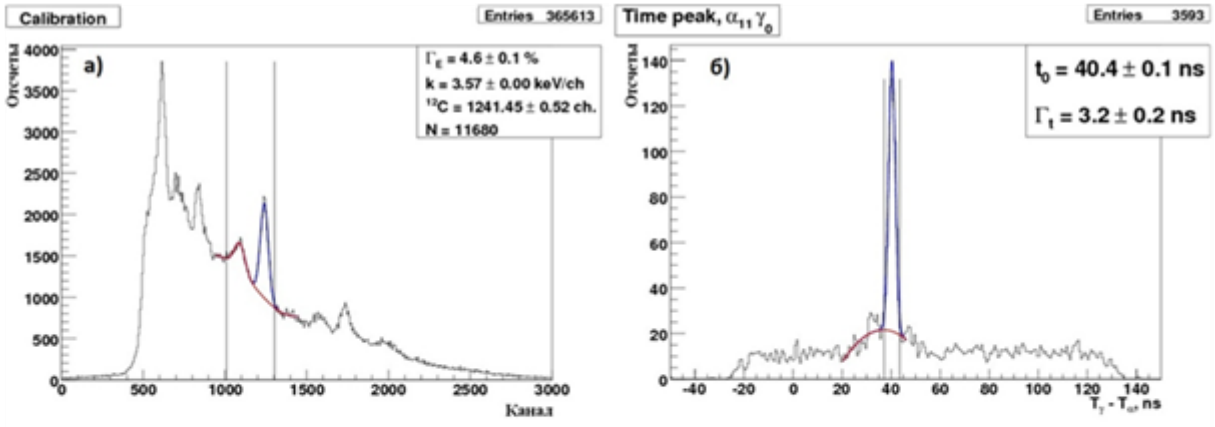

Fig. 5. Gamma-detector characteristics: a) amplitude distribution of events detected by a γ-detector at irradiation of pure ^{12}C sample by 14.1 MeV by a neutron flux. Vertical lines indicate γ-ray energy interval corresponding to the range from 3927 to 4438 keV. The peak position and width were determined based on their approximation to the Gaussian function. The background under the peaks was described by a second degree polynomial equation; b) spectrum of time intervals between triggerings of γ- and α-detectors corresponding to the above-specified energy range of detected characteristic carbon nuclei radiation (vertical lines

An automatic system for compensation of light output temperature variation is implemented in the PELAN system [12]. A constant response of the detector was attained by variation of a gain factor of the recording electronics channel depending on the BGO temperature and with regard to the measured temperature dependence of its light output [16]. The accuracy of response stabilization in this method was 7% at temperature variation from -5 to +45 °C.

The inspection systems developed and manufactured in the Joint Institute for Nuclear Research employ the program method of γ-detector response correction. It is easy to implement and adjust, applicable to a large number of detection channels and, except the BGO temperature measurement system, dose not require additional equipment. Correction of a signal from a γ–detector is based on the measurement of dependence of the response amplitude on the indication of the temperature sensor installed on the BGO crystal.

The investigation of temperature dependence of the γ–detector response was carried out in the climatic chamber in a temperature range from -20 to +55 °C. Standard ^{137}Cs и Co^{60} sources were used as γ–ray sources. The duration of detector calibration attained 45 hours and included four phases: detector cooling to -20 °C at a rate of 10 °C/h, spontaneous heating to room temperature, heating to +55 °C at a rate of 10 °C/h and spontaneous cooling (Fig. 6). The crystal temperature and the amplitude spectrum of γ-detector triggerings were recorded by the data reception and analysis system every 20 s. As shown in Fig. 6, when a BGO crystal is cooled to -20 °C, a relative deviation of ^{60}Co peak from the initial one is +30% at room temperature, crystal heating to +50 °C, on the contrary, shifts the peak towards small amplitudes by 40%.

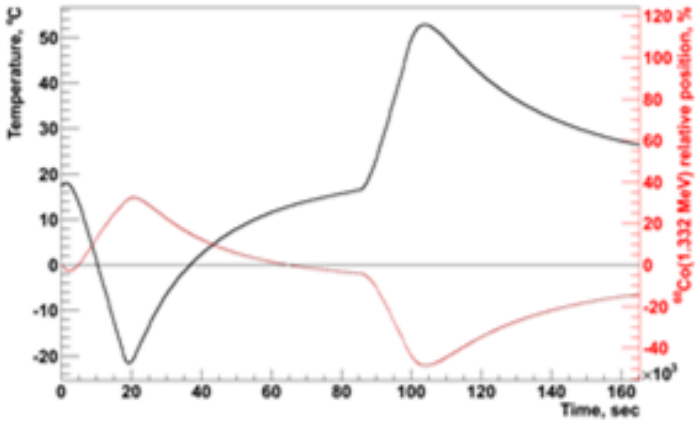

Figure 6. Crystal temperature (thick line, scale on the right) and deviation of 60Co (1.333 MeV) peak position (line, scale on the right) depending on the time from the beginning of calibration

The factor of conversion of the γ–ray energy into the amplitude spectrum channel number K_i was restored by the ^{137}Cs and ^{60}Co peaks for each time interval i. K_i dependence of the temperature T_i was described by a third degree polynomial equation of the type $F(T) = N*(1+\sum_{n=1}^{3} P_n * T^i)$, where P_n - polynomial factor and N - normalizing constant. The polynomial parameters were determined through minimization of a functional $\chi^2 = \sum_{i=1}^{m} \frac{(K_i - F(T_i))^2}{\delta K_i^2 + \delta F_i^2}$, where m - measurement number, δK_i - factor restoration error, δF_i - temperature-dependent T_i and its measurement error δT_i function variation $F(T)$. The sequence $F(T_i)$ describes K_i with accuracy better than 4%, the deviation is the maximum at the transit from heating to cooling and vice versa, which is

explained by the temperature gradient inside the massive crystal and the temperature T_i is measured on the crystal boundary.

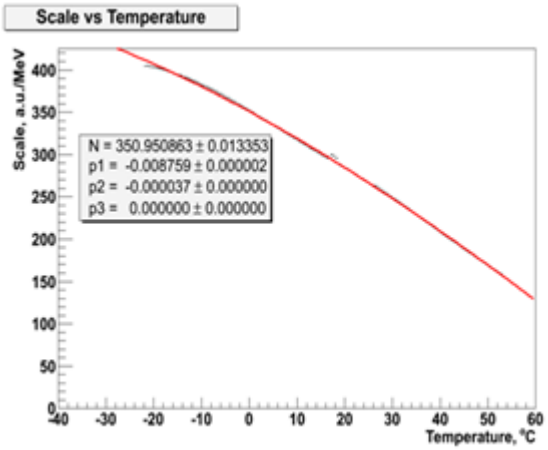

Fig. 7. The measured (dots) and parameterized (line) temperature dependence of the factor of energy conversion into the amplitude spectrum channel number

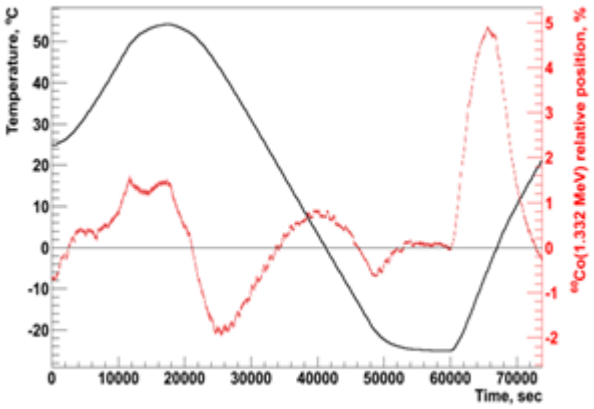

Fig. 8. Crystal temperature (thick line, scale on the left) and corrected deviation of 60Co (1.333 MeV) peak position (line, scale on the right) depending on the time from the beginning of the measurement

Fig. 7 shows the parameterized temperature dependence of the factor of conversion of the γ-ray energy into $F(T)$ the spectrum channel number. The function $F(T)$ describes the measured temperature dependence $K(T)$ obtained through averaging K_i values over the temperature interval from *T-0.25* to *T+0.25* °C with accuracy better than 2%.

Multiplication of γ-detector response by the function $F(T_o)/F(T)$, where T_o - specifies temperature normalization, compensates for temperature variation of the light output. The correction algorithm was tested in the climatic chamber with normalization for T_o = 20 °C. As shown in Fig. 8, variations of the γ-detector response did not exceed 2% at crystal cooling from +55 to -20 °C. The deviation maximum amounted to 5% at the beginning of spontaneous heating of a crystal up to room temperature and after switching off the chamber cooler.

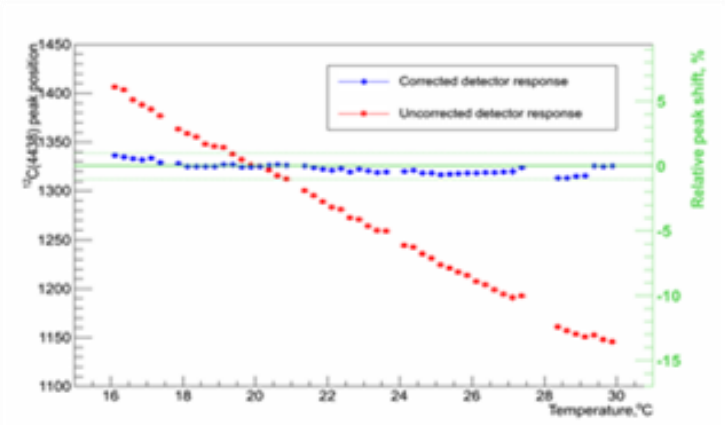

Fig. 9. ^{12}C peak position in the amplitude spectrum of a corrected and an uncorrected response of γ-detector depending on the crystal temperature

Fig. 9 shows the result of application of γ-detector response program stabilization in the DVIN-1 hand-held inspection system [3]. Due to heat generation of the operating neutron generator and the recording electronics the γ-detector was heated from 16°C to 30°C for the time of its work. When the crystal temperature was changed by 14°C, a relative deviation of the ^{12}C (E_γ=4438 keV) peak in the uncorrected spectrum amounted to ~20 %, whereas in the corrected data its deviation from the position at 20 °C does not exceed ±1%.

5. Conclusions

High efficiency of γ-rays detection, mechanical strength and radiation resistance of BGO crystals dictated our choice in favor of this scntillator in manufacture of γ-detectors for systems for hidden explosive and drug detection and identification. BGO gamma-detector displays excellent response linearity. The energy resolution of the detector on the 4438 keV line of carbon amounts to 4.5% at the time resolution of (α-γ)-coincidence detection system – 3.2 ns. Stability of detector energy calibration in the temperature range from -20 to +55 °C is provided by the developed method for γ-detector response temperature correction. This method is currently applied in all setups developed at JINR and ensures stability of energy calibration at the level of 2% that is sufficient for trustworthy detection of explosives and drugs in a wide temperature range.

References

1. Bystritsky V.M. et al. DViN - stationary setup for identification of explosives // Physics of Particles and Atomic Nuclei, Letters. 2008, Vol.5, No. 5, pp. 743-751.
2. Быстрицкий В.М. и др. Стационарный досмотровый комплекс ДВиН-2 // Письма в ЭЧАЯ. - Т.6. - №6. – 2009. - С. 586.
3. Сапожников М.Г. Детектор взрывчатых веществ ДВиН-1 для нужд транспортной безопасности // Транспортная безопасность и технологии. - № 2 (29). – 2012. - С. 169.
4. Bystritsky V.M. et al. Portable Neutron Generator with 9-Section Silicon α-Detector // Preprint of the Joint Institute for Nuclear Research E13-2006-36, Dubna, 2006.
5. Акимов Ю.К. Фотонные методы регистрации излучений. - Дубна: Объединенный институт ядерных исследований, 2006.
6. M. Globus, B. Grinyov, Jong Kyung Kim Inorganic Scintillators for Modern and Traditional Applications — Kharkiv : Institute for Single Crystals, 2005.
7. Обзор отечественных радиометрических и спектрометрических систем, которые могут быть использованы для целей учета и контроля ядерных материалов // [ФГУП «Всероссийский научно-исследовательский институт автоматики им. Н.Л.Духова»] URL: http://www.vniia.ru/rgamo/literat/obzor/doc/obzorrus.pdf.
8. J. Beringer et al. Particle Data Group // Phys. Rev. D86, 010001 (2012).
9. B. Perot et al. // Nucl. Instr. and Meth. B, 261 (2007), p. 295.
10. G. Perret et al. // J. Phys.: Conf. Ser. 41 375 (2006).
11. M. Gierlik at al. // IEEE TRANSACTIONS ON NUCLEAR SCIENCE, VOL. 53, NO. 3, JUNE 2006, p.1737.
12. R. Sullivan, "An Advanced ESTCP PELAN System for Surface and Near-surface UXO Discrimination", FINAL REPORT April 2007.
13. C. Eleon et al. // Nuclear Instruments and Methods in Physics Research A629 (2011) 220–229.
14. TMP36: Техническое описание на английском // [Analog Devices] URL: http://www.analog.com/static/imported-files/data_sheets/TMP35_36_37.pdf.
15. M. Bosteels, R. Weill. // Nucl. Instr. and Meth. B 498 (2003) 165–189.

16. Phillip C. Womble et al. *PELAN* 2001: Current Status of the PELAN Explosive Detection System // Proceedings SPIE conference on Hard X-Ray and Gamma-Ray Detector Physics, San Diego 7/29-8/3/ (2001).